

RADIATION SCATTERING

PACS numbers: 42.25.Fx; 42.65.Re
DOI: 10.1070/QE2014v044n01ABEH015266

Subdiffraction field localisation in the scattering of femtosecond laser radiation by a dielectric microsphere

Yu.E. Geints, A.A. Zemlyanov, E.K. Panina

Abstract. **The time dynamics of the optical field was theoretically considered in the near-field diffraction zone in the scattering of a femtosecond laser pulse by a transparent spherical microparticle. The spatial region of field focusing by the particle (the 'photonic jet' zone) was investigated; the evolution of the jet shape and the peak intensity in this region were analysed. For the first time it was determined that an extremely tight optical field localisation to a subdiffraction size is possible at a certain (resonance) temporal stage of photonic jet development.**

Keywords: *light scattering, microparticle, pulsed laser radiation, photonic jet, diffraction limit.*

1. Introduction

Diffraction in optics is the main wave process which sets the limiting size for the localisation of an optical field in its scattering from an obstacle or its passage through a focusing system. For a collecting lens with a round aperture the diffraction limit for the focusing of radiation with a plane wavefront and a wavelength λ in a substance is a circle of diameter $D_f = 1.22\lambda/\sin\theta$ [1], where θ is the aperture angle of the lens. This classical diffraction limit was obtained under the assumption that after the lens the light wave freely propagates to the focal region through a distance much longer than λ, i.e. that the electromagnetic field diffraction is considered in the far-field zone. Meanwhile, there exist the near- and transition-field zones of diffraction near objects of different physical nature illuminated by optical radiation. In these zones the light field has a more complicated spatial structure and may be localised tighter than prescribed by the classical treatment. In particular, this effect underlies the operation of near-field microscopy devices [2] and the subwavelength field focusing in the excitation of plasmon polaritons at the surface of metallic objects [3].

One more way of obtaining extreme light field localisation is the use of symmetric transparent dielectric mesoscale objects (microspheres, cylinders, ellipsoids) as optical focusers, i.e. objects whose transverse dimensions exceed the scattered light wavelength by no more than an order of magnitude. When a light wave is incident on such an object, in the near-field diffraction zone in the geometrical shadow region there forms a narrow light structure termed a photonic nanojet (PNJ) [4, 5]. This PNJ may be close to diffraction-limited in the transverse dimension (of the order of a wavelength) and may persist almost without variation in shape for a distance equal to several radiation wavelengths in the medium. The PNJ is nothing more than the region of external focus of the light wave diffracted by a transparent particle [6]. However, owing to the strong near-field object effect this wave structure has dimensional characteristics untypical for an ordinary collecting lens. The region of light focusing by a micrometre-sized particle stretches anomalously along the direction of radiation incidence to acquire the shape of a light jet produced by the interference of the waves transmitted through and refracted by the particle. A comprehensive review concerned with the theoretical and experimental research on the PNJ effect is found in Ref. [7].

The problems of enhancing the longitudinal and transverse localisation of the optical field in a PNJ were considered in several works with the corresponding variations in particle size and refractive index [8, 9], internal structure (gradient inhomogeneous refractive index [10, 11] and shape (ellipsoids [12]) or with the use of resonator properties of transparent microspheres [13, 14]. In the latter case, by way of exciting the natural structural (morphological) resonance of a dielectric sphere [15] by incident radiation it is possible to obtain an anomalously narrow PNJ near the particle due to the decaying eigenmode field 'leaking' through the surface.

At the same time, the resonance excitation of internal optical field in a particle is an intricate technical problem by itself and may require either a precision matching of the microsphere radius to the incident radiation wavelength or the use of a spectrally tunable radiation source for a given size of the available particle. The reason lies with the rather narrow spectral profile of the resonance mode, whose width is inversely proportional to the Q factor of the mode itself. Specifically, the halfwidth of the typical natural resonance of a two-micrometre quartz microsphere with a Q factor of ~5000 irradiated by the second harmonic of Nd:YAG laser radiation ($\lambda = 0.532$ μm) amounts to only 5 nm [14].

Zemlyanov and Geints [16] proposed the use of an ultrashort (femtosecond) laser pulse, which is initially spectrally broad, for the resonance excitation of the optical field of a microsphere. It turns out that the scattering of such a pulse by the particle almost always results in the resonance excitation of the internal optical field, when the eigenfrequencies of one or several high-Q resonance modes of the particle fall within the central part of the initial radiation spectrum. The PNJ formed under this pulsed irradiation scenario also turns out to be transient and generally comprises nonresonance and resonance time phases [17]. At the stage of resonance scatter-

Yu.E. Geints, A.A. Zemlyanov, E.K. Panina V.E. Zuev Institute of Atmospheric Optics, Siberian Branch, Russian Academy of Sciences, pl. Akad. Zueva 1, 634021 Tomsk, Russia; e-mail: ygeints@iao.ru, zaa@iao.ru, pek@iao.ru

Received 16 June 2013; revision received 2 October 2013
Kvantovaya Elektronika **44** (1) 48–53 (2014)
Translated by by E.N. Ragozin

ing there occur excitation and de-excitation of oscillation eigenmodes in the microparticle. It is significant that the transverse PNJ width at this stage of development becomes almost two times smaller than its stationary value and approaches the diffraction limit quite closely. This is at the expense of a significant lowering in intensity in the zone of a transient PNJ.

In the present work we continue the investigations commenced in Ref. [17], which are concerned with the temporal dynamics of a PNJ emerging in the scattering of ultrashort laser radiation by a transparent spherical microparticle. Using numerical simulations we show that the late phases of PNJ development are characterised by a tight subdiffraction spatial localisation of the optical field near the particle.

2. Temporal dynamics of PNJ development

We consider the linear scattering of a short laser pulse by a micrometre-sized nonabsorbing quartz microsphere. For definiteness, we select the carrier radiation wavelength $\lambda_0 = 0.4$ μm, the model microparticle radius a_0 is taken equal to 2.5 μm, and the particle itself is placed in the air (the refractive index $n_m = 1$). In what follows the particle and the ambient medium are assumed to be nonabsorbing. The duration t_p of a transform-limited Gaussian radiation pulse incident on the particle is assumed to be equal to 10 fs, which gives a relative profile halfwidth $\Delta\omega/\omega_0 \simeq 0.15$ (ω_0 is the central pulse frequency) broad enough to ensure the excitation of high-Q structural resonances of the particle field. The radiation is a plane wave in the direction transverse to that of pulse propagation.

This choice of particle and radiation parameters is not the only possible one, because realisation of the effect of PNJ formation necessitates only that the dimensionless parameter (the particle diffraction parameter) $x_a = 2\pi a_0/\lambda_0$ is in the value range $10 < x_a < 35$ [18] corresponding to mesoscale particles. This is due to the fact that, on the one hand, the PNJ is not formed for smaller particles and, on the other, for larger particles the near-field region for optical radiation scattering (the region of jet formation) spreads out and therefore does not exhibit sufficient localisation characteristic for precisely the PNJ.

We make several remarks prior to setting forth the theoretical model and discussing the simulation data. First, since we consider the linear scattering of optical radiation by a micrometre-sized dielectric sphere, this imposes certain limitations on the energy parameters (energy, power) of the incident radiation to rule out the manifestations of the optical nonlinearity of the particle material. The strongest nonlinear-optical effects in a transparent dielectric like quartz are Kerr self-focusing and optical breakdown [19]. In the near-IR wavelength range, the energy threshold of optical damage to quartz is equal to 0.1–0.3 μJ, while the threshold power for self-focusing amounts to ~2 MW [19]. Since similar data for the visible range are missing from the literature, we take these values for an approximate estimate of the thresholds. For a particle of radius $a_0 = 2.5$ μm irradiated by a laser pulse with a duration $t_p = 10$ fs and a carrier wavelength $\lambda_0 = 0.4$ μm – the situation treated below – we obtain that the peak intensity I_0 may not exceed $\sim 10^{12}$ W cm^{-2}. Furthermore, considering the effect of internal optical field focusing by the particle surface, this figure, as will be seen below, must be lower by at least two orders of magnitude. Therefore, the condition for the absence of nonlinear effects in the pulse diffraction by a quartz particle is as follows: $I_0 < 10^{10}$ W cm^{-2}.

Second, apart from the consideration of nonlinearity in the scattering of ultrashort radiation by particles, the inclusion of their material frequency dispersion, which shows up in the wavelength dependence of the linear refractive index n_a may be of significance. This may result in variations of the focal power of the particle, which is proportional to the product $n_a(\lambda)a_0$. Estimates of the frequency dispersion of fused quartz made by the Sellmeier formula [20] suggest that the refractive index of quartz varies from 1.4650 to 1.4816 for the 10-fs long radiation pulse under consideration, which has a spectral profile with a halfwidth of ~100 THz. From the standpoint of aerosol scattering, this variation of the particle's refractive index is too small to lead to an appreciable spatial redistribution of the optical field. This permits us to neglect the dispersion properties of the particle material in the execution of simulations. The quartz refractive index n_a in the visible range was taken to be equal to 1.5.

To simulate the temporal dynamics of the optical pulse field in the diffraction by the particle, we take advantage of the so-called nonstationary Mie theory [21], which is an extension of the classical theory of plane wave scattering by a sphere (the Mie theory [15]) to the case of incidence of a short light pulse. In the framework of this approach, the time dependence of the optical fields is taken into account by going over to the spectral frequency (ω) space. In this case, the initial transient problem of wave packet diffraction by a dielectric particle reduces to the stationary problem of the scattering, by a sphere, of a set of monochromatic Fourier harmonics into which the incident broadband radiation may be decomposed. The scattering properties of the particle are characterised by the spectral response function $\boldsymbol{E}_\delta(\boldsymbol{r};\omega)$. A detailed description of the method employed and some examples of its numerical implementation are given, for instance, in Refs [16, 21]. Here, we restrict ourselves to a brief list of the key points of the nonstationary Mie theory and give expressions for the time-dependent optical field components of the scattered wave.

In our numerical simulations we used the following representation for the electric intensity of the linearly polarised incident plane wave:

$$\boldsymbol{\mathcal{E}}^{\mathrm{i}}(\boldsymbol{r};t) = \frac{1}{2}\left[\boldsymbol{E}^{\mathrm{i}}(\boldsymbol{r};t) + \left(\boldsymbol{E}^{\mathrm{i}}(\boldsymbol{r};t)\right)^*\right]$$

$$= \frac{1}{2}E_0\boldsymbol{e}_y g(\tau)\exp(\mathrm{i}\omega_0\tau) + \text{c. c.},$$

where $g(\tau)$ is the temporal pulse profile; E_0 is the real amplitude of the field; $\boldsymbol{r}$ is the position vector of a spatial point; $\boldsymbol{e}_y$ is a unit vector in the direction of the y; $\tau = t - (z + a_0)n/c$ is the retarded time; and c is the speed of light in vacuum. A dielectric spherical particle of radius a_0 is located at the origin, and the laser pulse which experiences scattering by the particle propagates along the positive direction of the z axis. Taken for the parameter n is the corresponding value of the refractive index of the particle or air, depending on the spatial coordinate $\boldsymbol{r}$ in which the field is calculated.

The time profile of the light pulse is defined by the Gaussian function $g(\tau) = \exp[-(\tau - t_0)^2/(2t_p^2)]$, where t_0 is the time delay of the pulse. For simplicity of notation, in what follows we shall omit the complex conjugate part in the complex field representation.

To calculate the optical field distribution of the particle and apply the results of stationary Mie theory, one should

first pass from time coordinates to spectral frequencies and represent the initial light pulse by its Fourier image:

$$\mathcal{E}^{\mathrm{i}}_{\omega}(\boldsymbol{r};\omega) = \Im[\mathcal{E}^{\mathrm{i}}(\boldsymbol{r};t)] = \frac{1}{2}E_0\boldsymbol{e}_y G(\omega-\omega_0)\exp[-\mathrm{i}k_0 n(z+a_0)],$$

where

$$\Im[f(t)] = \int_{-\infty}^{\infty} f(t)\exp(-\mathrm{i}\omega t)\,\mathrm{d}t$$

is the Fourier transform operator; $G(\omega)$ is the frequency spectrum of the initial laser pulse; and $k_0 = \omega_0/c$. On multiplication by the harmonic function $\exp(\mathrm{i}\omega\tau)$, this relationship will formally define the spectral component of the initial radiation pulse in the form of a monochromatic linearly polarised wave with an amplitude $A(\omega) = E_0 G(\omega-\omega_0)$.

The diffraction of this monochromatic wave by a spherical particle is described in the framework of stationary Mie theory, which leads to the following general expression for the complex envelope of the electric field: $\boldsymbol{E}(\boldsymbol{r};\omega) = \exp(\mathrm{i}\omega\tau)A(\omega)\boldsymbol{E}_{\delta}(\boldsymbol{r};\omega)$. Here $\boldsymbol{E}_{\delta}(\boldsymbol{r};\omega)$ represents infinite series written for all spectral frequencies ω of the initial pulse at each point in space $\boldsymbol{r}$. For the fields of scattered and diffracted waves the spectral response function is of the following form [15]:

$$\boldsymbol{E}_{\delta}(\boldsymbol{r};\omega)=\begin{cases}\sum\limits_{l=1}^{\infty} E_l[\mathrm{i}a_l(m_{\mathrm{r}},x_{\mathrm{a}})\boldsymbol{N}^{(3)}_{\mathrm{e}1l}(\boldsymbol{r})-b_l(m_{\mathrm{r}},x_{\mathrm{a}})\boldsymbol{M}^{(3)}_{\mathrm{o}1l}(\boldsymbol{r})], & |\boldsymbol{r}|>a_0,\\ \sum\limits_{l=1}^{\infty} E_l[c_l(m_{\mathrm{r}},x_{\mathrm{a}})\boldsymbol{M}^{(1)}_{\mathrm{e}1l}(\boldsymbol{r})-\mathrm{i}d_l(m_{\mathrm{r}},x_{\mathrm{a}})\boldsymbol{N}^{(1)}_{\mathrm{o}1l}(\boldsymbol{r})], & |\boldsymbol{r}|\leqslant a_0.\end{cases} \quad (1)$$

Here $m_{\mathrm{r}} = n_{\mathrm{a}}/n_{\mathrm{m}}$ is the relative refractive index of the particle; $E_l = E_0\mathrm{i}^l(2l+1)/[l(l+1)]$ are the coefficients of incident wave expansion in terms of spherical harmonics; $\boldsymbol{M}^{(q)}_{\mathrm{e}1l(\mathrm{o}1l)}$ and $\boldsymbol{N}^{(q)}_{\mathrm{e}1l(\mathrm{o}1l)}$ are vector spherical harmonics; index l is the polar harmonic number; index q is the kind of the spherical Bessel function which enters in the expression for the harmonic; and the subscripts 'e' and 'o' correspond to the even and odd character of harmonic variation in azimuth angle. The values of partial coefficients a_l, b_l, c_l, and d_l depend on the relative refractive index m_{r} of the particle and on its optical dimension (diffraction parameter) $x_{\mathrm{a}}(\omega) = a_0\omega/c$ and are calculated by the well-known recurrent schemes.

The resultant nonstationary optical field (scattered and internal) is written in the form of the convolution of spectral functions (1), the frequency spectrum of the initial laser pulse, and its harmonic filling:

$$\boldsymbol{E}(\boldsymbol{r};\tau) = E_0\{\exp(\mathrm{i}\omega\tau)\boldsymbol{E}_{\delta}(\boldsymbol{r};\omega) * G(\omega)\}(\omega_0).$$

Here, expression $\{f(\omega)*h(\omega)\}(\omega_0)$ denotes an integral convolution operator.

We address ourselves to Fig. 1, which shows the sequential temporal stages of pulse scattering by the particle. Plotted in each frame is the two-dimensional distribution of the relative intensity $B(x,z) = |\boldsymbol{E}(x,y=0,z)|^2/E_0^2$ of the optical wave in the vicinity of the particle at some selected points in time. The radiation is incident from the top down. Every frame shows the spatial domain of area 100 μm^2 cut in the equatorial particle section in the plane of incident wave polarisation. For ease of perception, intensity B is additionally normalised to its maximum value $B_{\max}$ (shown in the upper right corner of each frame) realised at the corresponding point in time.

We consider in greater detail the temporal intensity behaviour in the spatial zone which comprises the PNJ domain. As is evident from Figs 1a–1c, on encountering the particle the radiation pulse experiences diffraction and then forms the zone of external concurrent focus in the shadow region of the

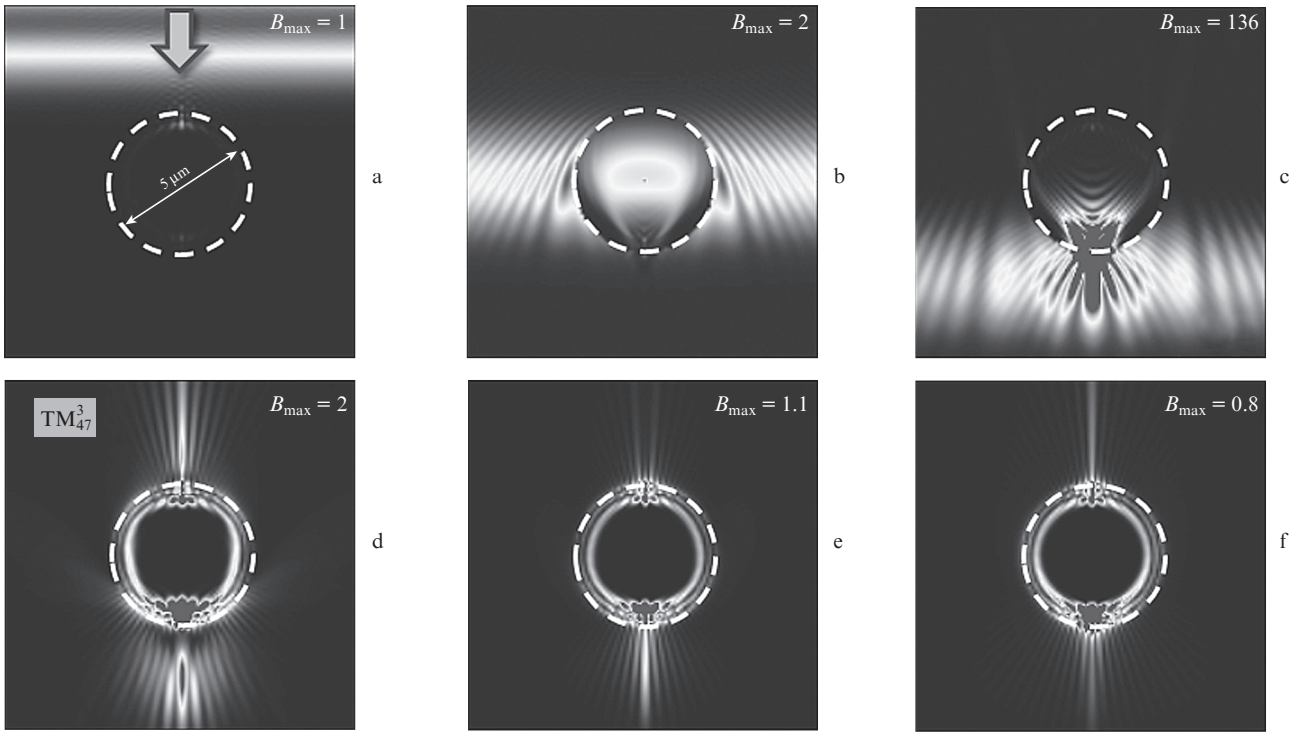

Figure 1. Normalised intensity distribution $B/B_{\max}$ in the vicinity of a spherical quartz particle illuminated by a laser pulse at the points in time t = (a) 30, (b) 70, (c) 100, (d) 170, (e) 240 and (f) 310 fs. The dashed circles indicate the particle surface. The image dimensions are 10×10 μm.

particle approximately 100 fs after the start of computation. This zone is the PNJ domain, which is subsequently referred to as the concurrent primary PNJ (PPNJ) and is characterised by sufficiently high peak intensities ($B_{max} > 100$). The spatial shape of this PPNJ at the point in time $t = 103$ fs, which is shown in Fig. 2a, is little different from that under stationary particle irradiation [17]. The field intensity distribution also has a principal maximum located in the immediate vicinity of the parent particle surface (shown with a dashed circumference) and feeble side lobes. They are produced by the interference of different parts of the light wave refracted by the spherical surface and make up the halo of the aberration focusing disc [1] in the near-field scattering zone.

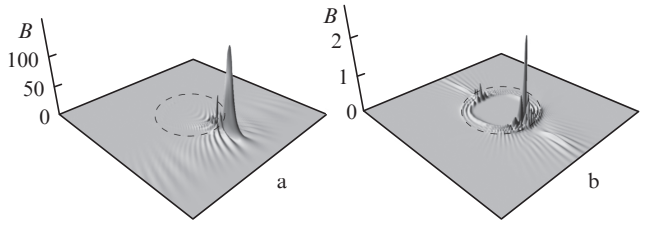

Figure 2. Volume spatial distribution of the relative intensity B in the PPNJ (a) and SPNJ (b) regions. The spatial image dimensions correspond to Fig. 1.

Figure 3a shows the temporal dynamics of the intensity $B(t)$ at the point of the absolute PPNJ field maximum. For the parameters selected, this point corresponds to a radial coordinate $r = 2.87$ μm in the particle shadow region (a polar angle $\varphi = 180°$). One can see that in approximately 140 fs the laser pulse leaves the computational domain, which measures two particle diameters, and the peak PNJ intensity becomes lower than $B_{max} \sim 10^{-3}$.

Subsequently, as follows from Fig. 3a, there again occurs an intensity increase at the selected point in space. The second intensity peak is attained for $t \approx 170$ fs, and then the intensity lowers again in a time corresponding to the incident pulse duration. As shown in Ref. [17], this one and the following decaying intensity oscillations in the PPNJ domain are due to a delay of a certain energy fraction of the scattered pulse in the excited high-Q particle eigenmodes. Therefore, upon PPNJ formation the particle is capable of generating additional spatially localised light structures in the form of a jet – secondary PNJs (SPNJs). These jets are lower in intensity, which depends on the Q factor of excited resonances.

Concerning the case under consideration, in the spectral response $S(\lambda) = |\boldsymbol{E}_\delta(a_0, \lambda)|^2$, which is shown in Fig. 3b, one can see several structural resonances centred within the spectral profile of the incident radiation (the hatched domain). The spectral halfwidths and intensities of these resonance modes are different and, in principle, they all may be simultaneously excited by the laser pulse. At the same time, the very shape of the spatial intensity distribution of the interior particle field in the form of two peaks connected by three nested rings (see Figs 1d and 2b) suggests that the resonance stage of scattering is dominated by the oscillation mode of third radial order. Real candidates for the formation of this internal field structure are the TM^3_{47}, TM^3_{48}, and TE^3_{47} modes located near the central pulse frequency (Fig. 3b). Higher-Q natural resonances, for instance the second-order modes TE^2_{46} and TE^2_{48}, are also excited, but the light energy captured by these modes

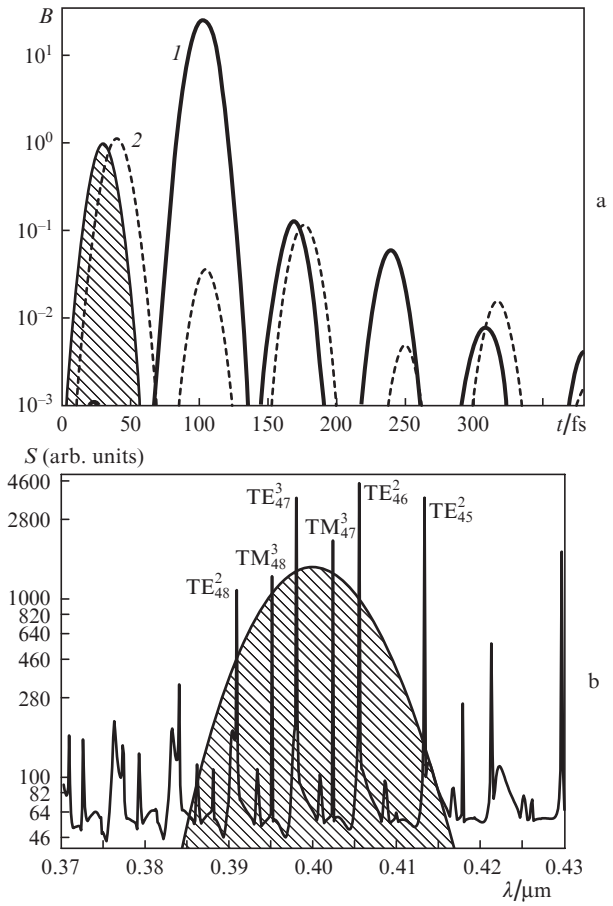

Figure 3. Time dependences of the relative intensities B in the domains of concurrent (*1*) and counter-propagating (*2*) PNJs (a) as well as spectral response (b) of a model quartz sphere illuminated by a laser pulse. The hatched domains show the pulse shape (a) and spectrum (b).

is much lower due to their remoteness from the centre of the spectral profile. That is why their radiation is masked by lower-Q but higher-power third-order modes.

A distinctive feature of the resonance temporal stage of pulse scattering (see Figs 1d–1f) is the emergence, apart from the ordinary concurrent PNJ, of a counter-propagating PNJ in the spatial intensity distribution, which is directed in opposition to the initial incident radiation. These SPNJs are similar in shape, intensity, and temporal dynamics, which is due to the common physical nature of their origin: the radiative loss of the eigenmode energies through the surface of the dielectric particle. In accordance with causality principle, the radiative loss of mode energy takes place primarily at the antinodes of the optical field in the illuminated and shadow hemispheres of the particle as evidenced by the large number of side lobes in the SPNJ zones in Fig. 2b. The spatial characteristics of the generated photon fluxes change due to the circumstance that the spherical particle at the late, resonance stage of scattering is no longer an optical focuser for the incident radiation (since it is no more) and plays the part of an open optical resonator.

Figure 4 shows the transverse intensity profiles of the optical field near the surface of the quartz particle (at a distance $\Delta z = +2a_0$) at the points in time corresponding to the intensity peaks of the PPNJ ($t = 100$ fs) and SPNJ ($t = 170$ fs). Each profile is normalised to its peak value. It will be recalled that that the 3-D image of these PNJs is shown is Figs 2a and 2b.

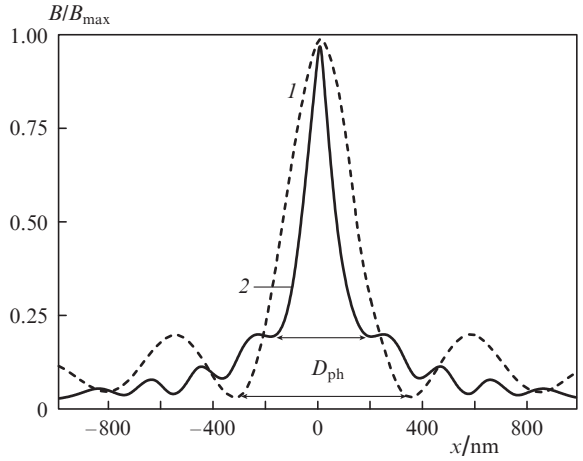

Figure 4. Normalised intensities of the optical field in the PPNJ (*1*) and SPNJ (*2*) domains near the surface of a quartz sphere.

One can see from Fig. 4 that the PPNJ and SPNJ have different spatial intensity distributions and above all different principal peak widths D_{ph}. If this parameter is defined by analogy with the diffraction width of a lens focal spot (the diameter of the Airy circle), i.e. as the distance between the first at-focus intensity minima, according to Fig. 4 we then have $D_{ph} \approx 600$ nm for the PPNJ and an almost two-times lower value $D_{ph} \approx 360$ nm for the SPNJ. We compare these values with the classical diffraction limit D_f of light wave focusing. For the limiting aperture angle $\theta = \pi/2$ we obtain $D_f \approx 490$ nm. Consequently, the width of the PPNJ, which is produced by the transmitted laser pulse, exceeds this limit by about 20%, while the size of the SPNJs, which are formed by the eigenmode radiation, becomes subdiffractional.

It should be realised that in the latter case we are not dealing with the field focusing by an optical system in the classical sense of this concept. The SPNJ production is the field radiation by particle resonance modes excited by the initial pulse. However, from the standpoint of spatial light field localisation it is of no fundamental significance how this localisation is achieved – with the use of focusing lenses or near-field effects or mode radiation from a resonator.

The SPNJ width D_{ph} is related to the linear dimension of the radiating aperture, which is formed by the antinodes of the electromagnetic field of an eigenmode. Figure shows a magnified image of the TM_{47}^3 mode field formed by the point in time $t = 170$ fs. One can see three concentric rings, in which the internal field of the mode is confined, and the external PNJ domain. The inner ring consists of intensity peaks uniformly distributed over the polar angle; their number N is determined by the number l of the excited structural resonance: $N = 2l$ [22]. The width (aperture) d of every peak is calculated as the ratio between the inner ring circumference and the number of peaks: $d = \pi a_3/l$, where a_3 is the ring radius.

We put $a_3 \approx a_0$ and use an analytical relation to calculate the particle's resonance diffraction parameter for the eigenmode TM_l^q [23]:

$$\frac{n_a}{n_m} x_{al}^{(q)} \approx (l + 1/2)\left[1 + 2^{-1/3}\alpha_q (l + 1/2)^{-2/3}\right] + O(l^{-4/3}),$$

where α_q is the qth root of the Airy function. On simple rearrangement we obtain

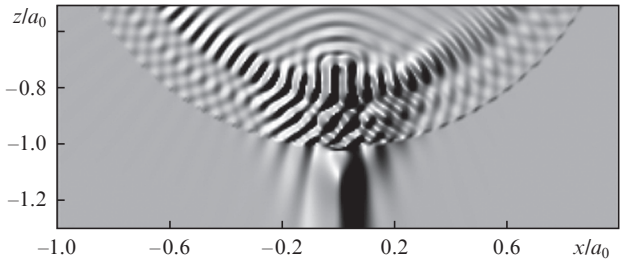

Figure 5. Magnified image of the spatial intensity distribution of the TM_{47}^3 eigenmode of a quartz particle ($a_0 = 2.5$ μm).

$$d \approx \frac{\lambda n_m}{2n_a}\left[1 + 2^{-1/3}\alpha_q (l + 1/2)^{-2/3}\right]. \quad (2)$$

This relationship defines the peak width of the intensity distribution of the natural resonance of a dielectric sphere and gives the approximate linear size of the light structure radiated outside from the domain of this peak. We substitute the specific values $l = 47$, $q = 3$, $\alpha_q = 5.52$, $\lambda = 397$ nm (the resonance wavelength), $n_a = 1.5$, $n_m = 1$ and take into account that the SPNJ width $D_{ph} \approx 2d$ (Fig. 5) to obtain the following estimate for the case under consideration: $D_{ph} \approx 380$ nm, which is in rather good agreement with the data of numerical analysis.

3. Conclusions

Therefore, our investigations into the temporal dynamics of the optical field in the region of a PNJ formed in the femtosecond pulsed illumination of a transparent microsphere allow a conclusion that the amplitude and spatial characteristics of the PNJs depend heavily on the nature of their origin. The PPNJ, which is formed in the focusing of the radiation pulse by the spherical particle, is characterised by a relatively high peak intensity and is hardly different in spatial shape from that produced under stationary particle irradiation. The SPNJs, which result from the radiative loss of excited eigenmode energies through the surface of the dielectric particle, are significantly lower in intensity, but they may be subdiffractional in transverse size. Tighter localisation of the PPNJ requires, as indicated by relationship (2), the excitation of higher-Q resonance modes (by increasing l and/or lowering q) and an improvement in the optical contrast n_a/n_m of the microsphere.

Acknowledgements. This work was supported by the Ministry of Education and Science of the Russian Federation under Agreement No. 8381.

References

1. Born M., Wolf E. *Principles of Optics* (Oxford: Pergamon Press, 1965; Moscow: Nauka, 1970).
2. Zhdanov G.S., Libenson M.N., Martsinovskii G.A. *Usp. Fiz. Nauk*, **168**, 801 (1998) [*Phys. Usp.*, **41** (7), 719 (1998)].
3. Zayats A., Smolyaninov I.I., Maradudin A.A. *Phys. Rep.*, **48**, 131 (2005).
4. Chen Z., Taflove A., Backman V. *Opt. Express*, **12**, 1214 (2004).
5. Heifetz A., Huang K., Sahakian A.V., Li X., Taflove A., Backman V. *Appl. Phys. Lett.*, **89**, 221118 (2006).
6. Itagi A.V., Challener W.A. *J. Opt. Soc. Am. A*, **22**, 2847 (2005).
7. Heifetz A., Kong S.-C., Sahakiana A.V., Taflove A., Backman V. *J. Comput. Theor. Nanosci.*, **6** (9), 1979 (2009).
8. Lecler S., Takakura Y., Meyrueis P. *Opt. Lett.*, **30**, 2641 (2005).

9. Geints Yu.E., Zemlyanov A.A., Panina E.K. *Opt. Spektrosk*., **109**, 643 (2010).
10. Kong S.-C., Taflove A., Backman V. *Opt. Express*, **17**, 3722 (2009).
11. Geints Yu.E., Zemlyanov A.A., Panina E.K. *Opt. Atmos. Okeana*, **24**, 617 (2011).
12. Mendes M.J., Tobias I., Marti A., Luque A. *Opt. Express*, **19**, 16207 (2011).
13. Heifetz A., Simpson J.J., Kong S.-C., Taflove A., Backman V. *Opt. Express*, **15**, 17334 (2007).
14. Geints Yu.E., Zemlyanov A.A., Panina E.K. *J. Opt. Soc. Am. B*, **29**, 758 (2012).
15. Bohren C.F., Huffman D.R. *Absorption and Scattering of Light by Small Particles* (New York: Wiley, 1983; Moscow: Mir, 1986).
16. Zemlyanov A.A., Geints Yu.E. *Opt. Spektrosk.*, **96**, 357 (2004).
17. Geints Yu.E., Zemlyanov A.A., Panina E.K. *Opt. Atmos. Okeana*, **25**, 1028 (2012).
18. Geints Yu.E., Panina E.K., Zemlyanov A.A. *Opt. Atmos. Okeana*, **25**, 417 (2012).
19. Couairon A., Myzyrowicz A. *Phys. Rep.*, **441**, 47 (2007).
20. Couairon A., Sudrie L., Franco M., Prade B., Mysyrowicz A. *Phys. Rev. B*, **71**, 125435 (2005).
21. Shifrin K.S., Zolotov I.G. *Appl. Opt.*, **34**, 552 (1995).
22. Lam C.C., Leung P.T., Young R. *J. Opt. Soc. Am. B*, **9**, 1585 (1992).
23. Geints Yu.E., Zemlyanov A.A., Zuev V.E., Kabanov A.M., Pogodaev V.A. *Nelineinaya Optika Atmosfernogo Aerozolya* (Nonlinear Optics of Atmospheric Aerosol) (Novosibirsk: Izd. SO RAN, 1999).